Photolysis of 2,3-pentanedione and 2,3-hexanedione: Kinetics, quantum yields, and product study in a simulation chamber

ARTICLE *in* ATMOSPHERIC ENVIRONMENT · JANUARY 2014

Impact Factor: 3.28 · DOI: 10.1016/j.atmosenv.2013.10.039

4 AUTHORS:

Hichem Bouzidi
Ecole des Mines de Douai
9 PUBLICATIONS **9** CITATIONS
SEE PROFILE

Christa Fittschen
CNRS - Université Lille 1
113 PUBLICATIONS **1,357** CITATIONS
SEE PROFILE

Patrice Coddeville
Ecole des Mines de Douai
55 PUBLICATIONS **404** CITATIONS
SEE PROFILE

Alexandre Tomas
Ecole des Mines de Douai
41 PUBLICATIONS **241** CITATIONS
SEE PROFILE

Atmospheric Environment 82 (2014) 250–257

Contents lists available at ScienceDirect

Atmospheric Environment

journal homepage: www.elsevier.com/locate/atmosenv

Photolysis of 2,3-pentanedione and 2,3-hexanedione: Kinetics, quantum yields, and product study in a simulation chamber

H. Bouzidi [a,b], C. Fittschen [a,c], P. Coddeville [a,b], A. Tomas [a,b,*]

[a] Univ. Lille Nord de France, F-59500 Lille, France
[b] Mines Douai, CE, F-59508 Douai, France
[c] PC2A – CNRS – Université Lille 1, F-59655 Villeneuve d'Ascq, France

HIGHLIGHTS

- Photolysis is the main atmospheric fate of the α-diketones investigated.
- Lifetimes of around 2.5 h have been calculated for both α-diketones.
- Effective quantum yields of about 0.2 have been determined.
- In the troposphere, photolysis occurs mainly through C(O)–C(O) bond scission.
- Carbonyl compounds are the principal photolysis products.

ARTICLE INFO

Article history:
Received 14 May 2013
Received in revised form
14 October 2013
Accepted 16 October 2013

Keywords:
Dicarbonyl
OVOC
Oxygenated Volatile Organic Compound
Atmosphere

ABSTRACT

The gas phase photolysis of two α-diketones, 2,3-pentanedione (PTD) and 2,3-hexanedione (HEX), has been studied in a Teflon simulation chamber using UV lamps in the 330–480 nm wavelength range. Photolysis rates have been determined at room temperature and atmospheric pressure. Using NO_2 actinometry allows estimating the lifetime of PTD and HEX in the atmosphere to be about 2.5 h, assessing the dominance of the photolysis loss process over the OH reaction for such α-dicarbonyl compounds. Effective quantum yields for PTD and HEX have also been calculated over the whole wavelength range: $\Phi_{PTD} = 0.20 \pm 0.02$ and $\Phi_{HEx} = 0.18 \pm 0.03$, consistent with literature values on α-dicarbonyls. Various end-products from the photolysis of PTD and HEX have been identified and quantified. For PTD, CH_2O and CH_3CHO have been detected with molar yields of $(48 \pm 0.5)\%$ and $(41 \pm 0.7)\%$, respectively. For HEX, CH_2O and C_2H_5CHO have been detected with molar yields of $(45 \pm 1.1)\%$ and $(37 \pm 0.8)\%$, respectively. Small amounts of CO have also been observed, with yields of about 2%, as well as organic acids. Experiments performed in the absence of OH-radical scavengers showed significantly faster photolysis rates and higher CO yields (~7%), indicating clear formation of OH radicals in the chemical systems. A reaction mechanism was developed for PTD and HEX photolysis based on the product observations, which allowed simulating the reactant and product time profiles with very good agreement. The present work represents the first study of 2,3-pentanedione and 2,3-hexanedione photolysis, to our knowledge, and may contribute to a better understanding of the photolysis of the α-diketones in the troposphere.

1. Introduction

Oxygenated Volatile Organic Compounds (OVOCs) constitute a large group of volatile organic compounds (VOCs) in the atmosphere, being emitted from various anthropogenic and biogenic sources and playing a significant role in atmospheric chemistry (Atkinson and Arey, 2003). Among numerous OVOCs, carbonyl species represent an important group, as they can be formed *in situ* in the atmosphere as the result of the atmospheric transformation of other VOCs and because of their high reactivity. In the course of the atmospheric oxidation of many VOCs like isoprene, aromatics, and alkenes, α-dicarbonyl compounds have been shown to be formed in relatively high yields (Calvert et al., 2002; Fu et al., 2008; Grosjean and Grosjean, 1998). A few studies indicate that these α-dicarbonyl compounds are short-lived species in the troposphere

* Corresponding author. Département Chimie et Environnement, Ecole Nationale Supérieure des Mines de Douai, 941 rue Charles Bourseul, CS 10838, F-59508 Douai Cedex, France. Tel.: +33 3 27 71 26 51; fax: +33 3 27 71 29 14.
E-mail address: alexandre.tomas@mines-douai.fr (A. Tomas).

1352-2310/$ – see front matter © 2013 Elsevier Ltd. All rights reserved.
http://dx.doi.org/10.1016/j.atmosenv.2013.10.039

with photolysis being the major elimination pathway, thus representing a direct source of radicals in the atmosphere (Calvert et al., 2011; Plum et al., 1983; Szabo et al., 2011; Tadic et al., 2006). Yet, the kinetics and mechanisms of α-dicarbonyl photolysis are not well known and discrepancies subsist especially in the quantum yields even for methylglyoxal, one of the simplest α-dicarbonyls (Sander et al., 2011). In spite of the importance of α-dicarbonyl compounds, literature data is very limited, especially for species >C4.

In this paper, we have focussed on the atmospheric chemistry of two α-diketones: 2,3-pentanedione ($CH_3C(O)C(O)CH_2CH_3$) and 2,3-hexanedione ($CH_3C(O)C(O)CH_2CH_2CH_3$) in order to extend our knowledge on α-dicarbonyl photolysis mechanisms. Apart from being emitted by wine industries (Campo et al., 2006), 2,3-pentanedione (PTD) and 2,3-hexanedione (HEX) have been identified as reaction products in the ozonolysis of alkenes. Indeed, PTD and HEX have been shown to originate from the oxidation of the carbonyl oxide Criegee biradical R_1R_2COO, where R_1R_2 = alkyl groups (Grosjean and Grosjean, 1998). For example, the ethyl–ethyl carbonyl oxide biradical (formed from 2-ethyl-but-1-ene ozonolysis) may rearrange into an unsaturated hydroperoxide to finally produce 2,3-pentanedione and H_2 (Grosjean and Grosjean, 1998):

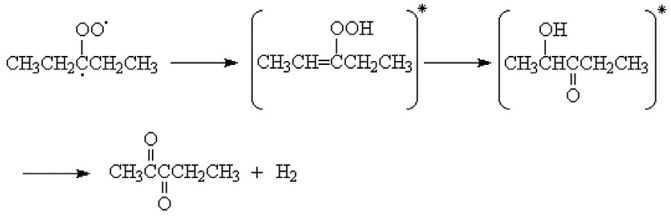

Advanced analytical analysis of secondary organic aerosols observed in the OH-initiated photo-oxidation of toluene also revealed the presence of PTD among many other dicarbonyls (Hamilton et al., 2005). Recent work performed in our laboratory on the kinetics of 2,3-pentanedione photooxidation showed that its tropospheric fate relies mainly on the photolysis reaction, with very short photolysis lifetime of about 1 h (Szabo et al., 2011), in agreement with biacetyl reactivity (Klotz et al., 2001). Two different experimental setups were employed by Szabo et al. (laser photolysis at 351 nm and Teflon chamber with broadband UV lamps) and a strong disagreement for the primary quantum yield was found between the two experimental setups (0.11 in laser photolysis and 0.41 in Teflon chamber). Furthermore, the observation of photolysis products was not reported. Thus, a more detailed characterization of the photochemical reactivity of α-diketones compounds is clearly needed to improve our understanding of the implication of these species in the chemistry of the atmosphere and allow further extension of atmospheric chemistry models for improvement of air quality predictions. The objective of this study was to investigate the kinetics and mechanisms of the photolysis of two α-diketones: 2,3-pentanedione and 2,3-hexanedione using a Teflon environmental simulation chamber.

2. Experimental section

2.1. Simulation chamber experiments

The photolysis experiments have been carried out in a 250 L FEP Teflon film chamber at room temperature (298 K) and in 1 atm of air. Details on the experimental setup can be found elsewhere (Szabo et al., 2009, 2011) and only few specific aspects will be described in the following. The chamber is equipped with twelve fluorescent tubes (Philips Sylvania/TLK) emitting in the 330–480 nm region with a maximum near 370 nm. The procedure for a typical experiment was as follows: After injection of the α-diketone, the reaction mixture was allowed to stand for about half an hour in the dark. Then, two samples are taken to determine the initial concentration of the reactant. After the second sampling, the lamps are switched on. About 10 samples are taken along the photolysis experiments (lasting 6–8 h) to monitor the concentration of α-diketone and end-products over time. Initial reactant concentrations were 12–48 ppm for PTD and 10–74 ppm for HEX. Some experiments have been performed in the presence of ethanol, cyclopentane or 1-pentene as scavenger of OH radicals, as these radicals may be released during reactions between peroxyl radicals (Dillon and Crowley, 2008; Jenkin et al., 2007). The scavenger concentrations were calculated such that more than 90% of the OH radicals react with the scavenger based on the known OH reaction rate constants of the reactants and scavengers.

2.2. Test experiments

Test experiments were carried out to investigate possible losses of reactants and products during the photolysis experiments. First, deposition rates on the chamber walls were tested for by running experiments in the dark for around 9 h. Results showed that such losses were negligible for the reactants and were very low for CH_2O, CH_3CHO and C_2H_5CHO (rates <1% per hour). Tests for possible losses of products through photolysis were also carried out. Results indicate that only CH_2O photolysis was significant with a loss rate of 2.1% per hour for 12 lamps, while the photolysis rates of other carbonyl products were found <1% per hour, consistent with the recommended absorption cross sections and quantum yields of the tested carbonyls (Sander et al., 2011). In the following, the concentrations of CH_2O, CH_3CHO and C_2H_5CHO have been corrected for wall deposition and photolysis according to the rates determined in the test experiments.

2.3. Sampling and analytical techniques

The concentrations of the reactants (PTD and HEX) were measured either by a thermodesorption – gas chromatographic (TD–GC) system coupled with Fourier Transform Infrared (FTIR) spectroscopy and Flame Ionization Detection (FID) or by FTIR spectroscopy using a White cell (2 L volume, optical path length of 10 m). The TD-GC-FTIR-FID analytical system is similar to that used in Turpin et al. (2006); briefly, 20 mL gas aliquots from the reaction chamber are cryotrapped at −200 °C in the TD (TCT Chrompack) before being flash injected in the GC (Perkin Clarus 500) and eluted in the column (CP Sil 5 CB, 50 m, 0.32 mm I.D.). Detection is provided by on-line FTIR spectrometry (Nicolet 6700 with MCT detector) followed by FID. Mid-IR spectra were recorded at a 16 cm^{-1} resolution every 0.56 s (4 interferograms average). In the case of the White cell, gas samples were withdrawn from the chamber and analyzed with the FTIR spectrometer (main bench with DTGS detector). IR spectra typically result from the co-addition of 100 scans with a resolution of 2 cm^{-1} representing a collection time of about 4 min. The spectral regions used for PTD and HEX analysis are between 948–857 cm^{-1} and 968–909 cm^{-1}, respectively, and their concentrations were determined by classical calibration procedures. The amount of CO was determined by the FTIR-White cell system via a quantitative analysis calibration technique based on the classical least squares algorithm (CLS) available in the TQ Analyst software (Thermo Fisher Scientific Inc.).

Carbonyl products were analyzed using 2,4-dinitrophenylhydrazine (DNPH) derivatization followed by HPLC-UV analysis of the hydrazones. DNPH-coated Sep-Pak silica

gel cartridges (Waters, USA) were used with a 2 min sampling time at 830 mL min^{-1}. The hydrazones were eluted from the cartridges with 4–6 mL acetonitrile and analyzed by HPLC-UV (Waters 2695, column C18, 25 cm × 4.6 mm × 5 μm at 40 °C) using an elution gradient stated at 1.5 mL min^{-1} (acetonitrile, water and tetrahydrofuran) and a UV–Visible detector at 365 nm (Dual λ 2487). Quantitative analysis involved the use of external standards prepared with carbonyl-DNPH derivatives synthesized in the laboratory. Calibrations curves were constructed and used to quantify the carbonyl concentrations in the sample collected. The total volume of gas extracted at the end of an experiment lay between 13 and 35 L, corresponding to 5% and 14% of the reaction volume. No impact of the sampling volume could be observed on the results.

2.4. NO_2 actinometry

NO_2 was used as actinometer in order to estimate the tropospheric photolysis lifetime and the effective quantum yields. The photolysis frequency of NO_2 (k_{NO_2}) in the simulation chamber was determined using the method developed by Holmes et al. (1973). Experimental details can be obtained in Djehiche et al. (2011). The k_{NO_2} value obtained for 12 lamps was 9.0 ± 0.4 h^{-1}, respectively. For comparison, on 1st July at midday under cloudless sky (40°N, optimized albedo), the photolysis frequency of NO_2 is 29 h^{-1} (Seinfeld and Pandis, 1998).

2.5. Chemicals

PTD (>97%), HEX (>93%) and cyclopentane (>99%) were purchased from Sigma–Aldrich, ethanol (>99.9%), acetonitrile (>99.7%) and water (>99.9%) from Merck, 1-pentene (>95%) from Riedel-de-Haën and tetrahydrofuran (THF) (>99.9%) from Acros Organics. All compounds were used as received without further purification. Pure, dry air was produced by a zero air generator (Claind AZ 2020). Pure NO_2 and CO (4939 ppmv in N_2) were obtained from Air Liquide and Praxair, respectively.

3. Results and discussion

3.1. Photolysis rate constants

The photolysis of PTD and HEX was carried out using 12 fluorescent lamps in the absence or presence of OH radical scavengers. The photolysis rate constants $k_{\alpha\text{-diketone}}$ were determined by plotting the natural logarithm of the ratio [α-diketone]$_0$/[α-diketone] versus time:

$$\mathrm{Ln}\frac{[\alpha-\mathrm{diketone}]_0}{[\alpha-\mathrm{diketone}]} = k_{\alpha-\mathrm{diketone}} \times t$$

[α-diketone]$_0$ and [α-diketone] are the concentrations of α-diketone (PTD or HEX) at times zero and t, respectively. As noticed on Fig. 1, the concentration data are well fitted to a straight line using a linear least-squares procedure and the slope of the linear regression (weighted by 1σ) leads to $k_{\alpha\text{-diketone}}$. The photolysis rate constants obtained for PTD (5 experiments) and HEX (2 experiments) in the presence of an OH radical scavenger are (0.129 ± 0.001) h^{-1} and (0.116 ± 0.004) h^{-1}, respectively. The reported uncertainties represent one standard deviation of the slope of the regression line.

Experiments performed in the absence of an OH radical scavenger gave photolysis rate constants of (0.155 ± 0.001) h^{-1} and (0.158 ± 0.001) h^{-1} for PTD (4 experiments) and HEX (4 experiments), respectively, corresponding to an increase of 20% and 36%.

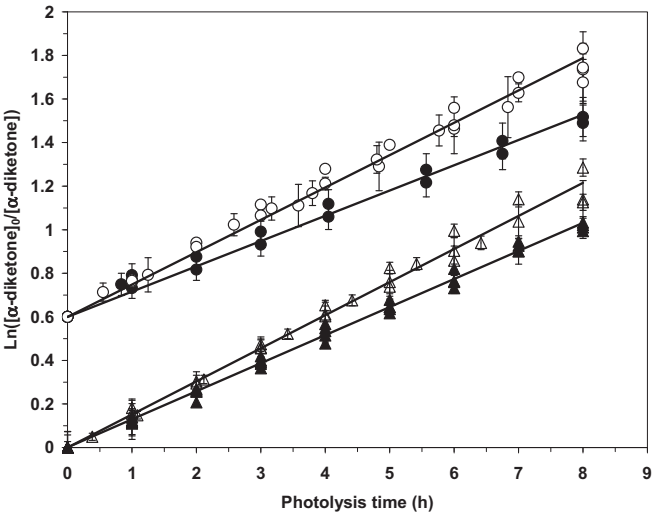

Fig. 1. Kinetics of PTD (△,▲) and HEX (○,●) photolysis. Empty symbols are for experiments without OH-scavenger, while full symbols are for experiments with OH-scavenger. Error bars correspond to statistical uncertainties (1σ). The HEX y-data have been shifted by +0.6 for clarity.

This increase reasonably points to the formation of OH radicals in the chemical mechanism, arising probably through peroxy radical reactions and reacting with PTD and HEX. A similar effect was observed by Szabo et al. (2011) in their PTD photolysis experiments using 312 nm lamps with an increase of ~37% of the photolysis rate constant in the absence of an OH radical scavenger. Using the PTD photolysis frequencies with and without scavenger and the OH + PTD rate constant (Szabo et al., 2011), a rough estimate of 1–2 × 10^6 cm^{-3} OH radical photostationary concentrations can be determined in the reaction system.

3.2. Effective quantum yields

From the obtained photolysis frequencies, the effective quantum yields for PTD and HEX can be retrieved using NO_2 actinometry experiments according to the following equation (Plum et al., 1983):

$$\Phi_{\alpha-\mathrm{diketone}} = \frac{k_{\alpha-\mathrm{diketone}}/k_{NO_2}}{k^{\mathrm{calc}}_{\alpha-\mathrm{diketone}}/k^{\mathrm{calc}}_{NO_2}} \quad (1)$$

$k^{\mathrm{calc}}_{\alpha-\mathrm{diketone}}$ and $k^{\mathrm{calc}}_{NO_2}$ are the calculated α-diketone and NO_2 photolysis rate constants, respectively. They are determined using

$$k^{\mathrm{calc}}_{\alpha-\mathrm{diketone}} = \int_{\lambda} \Phi_{\alpha-\mathrm{dk}}(\lambda)\sigma_{\alpha-\mathrm{dk}}(\lambda)F(\lambda)\mathrm{d}\lambda \quad (2)$$

and

$$k^{\mathrm{calc}}_{NO_2} = \int_{\lambda} \Phi_{NO_2}(\lambda)\sigma_{NO_2}(\lambda)F(\lambda)\mathrm{d}\lambda \quad (3)$$

$\Phi_{\alpha\text{-dk}}(\lambda)$ and $\Phi_{NO_2}(\lambda)$ represent the α-diketone and NO_2 wavelength-dependent quantum yields, $\sigma_{\alpha\text{-dk}}(\lambda)$ and $\sigma_{NO_2}(\lambda)$ the α-diketone and NO_2 absorption cross sections and $F(\lambda)$ the relative actinic flux intensity. The relative emission spectrum was recorded using a spectroradiometer (SolaTell) with a spectral resolution 0.5 nm. PTD absorption cross-sections were from Szabo et al. (2011) and PTD quantum yields in Equation (2) were set to unity. The HEX absorption cross-sections were assumed to be similar to those of

Table 1
Product yields (corrected for wall loss and photolysis) determined from the slopes of the plots of Fig. 2a and b in the absence and presence of OH radical scavengers (errors are 1σ and represent the statistical uncertainty on the linear regression only).

α-diketone	Scavenger	Product yields (%)			
		CH_2O	CH_3CHO	C_2H_5CHO	CO
PTD	No	41 ± 0.7	39 ± 0.6	–	7.6 ± 0.5
	Yes[a]	48 ± 0.5	41 ± 0.7	–	2.6 ± 0.1
HEX	No	42 ± 0.6	–	30 ± 0.5	7.1 ± 0.1
	Yes[b]	45 ± 1.1	–	37 ± 0.8	1.7 ± 0.3

[a] 1-pentene, ethanol and cyclopentane have been used. CH_2O yields are from experiments with ethanol and cyclopentane, while CH_3CHO yields are from experiments with 1-pentene and cyclopentane.
[b] Cyclopentane only used as scavenger.

PTD and HEX quantum yields were also set to unity. $\Phi_{NO_2}(\lambda)$ and $\sigma_{NO_2}(\lambda)$ were from Atkinson et al. (2004).

The experimental $k_{\alpha\text{-diketone}}/k_{NO_2}$ ratios obtained are 0.014 ± 0.001 and 0.013 ± 0.001 for PTD and HEX, respectively, where stated uncertainties represent 1σ. These values compare fairly well with the ratio obtained by Plum et al. (1983) for methylglyoxal (0.019) using a xenon arc solar simulator. They are however a factor of two lower than the ratios obtained for biacetyl (0.036) (Plum et al., 1983; Klotz et al., 2001). Using Equation (1), the effective quantum yields for PTD and HEX can be calculated: $\Phi_{PTD} = 0.20 \pm 0.02$ and $\Phi_{HEx} = 0.18 \pm 0.03$. Note that these yields are strictly speaking only applicable to the irradiation source used in the present work and can be considered as upper limits for the atmosphere. The main sources of uncertainties are the PTD absorption cross-sections and the experimental PTD, HEX and NO_2 photolysis frequencies, yielding an overall uncertainty of 12% on the PTD effective quantum yield, maybe slightly higher for HEX as the cross sections are not known. The effective quantum yields determined in the present work agree quite well with the yield determined by Szabo et al. (2011) using the 351 nm laser light (0.11) while a bit lower than the yield determined using the UV broadband lamps at 312 nm where higher-energy channels can occur (0.41). For comparison, the recommended glyoxal photolysis quantum yield at 370 nm is 0.316, varying from 1 to 0 between 330 nm and 440 nm (Sander et al., 2011), while methylglyoxal photolysis quantum yields range from 0.78 (330 nm) to 0 (440 nm) with a value of 0.17 at 370 nm (Koch and Moortgat, 1998).

3.3. Photolysis products

The major photolysis products observed are formaldehyde (CH_2O) and acetaldehyde (ACT) in the PTD photolysis, and formaldehyde and propanal (PRP) in the photolysis of HEX. They arise from the well-known reactivity of the CH_3CO, C_2H_5CO and C_3H_7CO acyl radicals produced in the primary photolysis reaction steps:

$CH_3C(O)C(O)C_2H_5 + h\nu \rightarrow CH_3CO + C_2H_5CO$ ($\lambda < 402$ nm, Kercher et al., 2005; Sander et al., 2011)

and

$CH_3C(O)C(O)C_3H_7 + h\nu \rightarrow CH_3CO + C_3H_7CO$

In the presence of O_2, CH_3CO, C_2H_5CO and C_3H_7CO radicals partly lead to CH_2O, CH_3CHO and C_2H_5CHO respectively, involving successive radical reaction steps (see also Table 2) of alkyl peroxy and alkoxy radicals (Lesclaux, 1997) that can be resumed in:

$CH_3CO \rightarrow CH_3C(O)O_2 \rightarrow CH_3 \rightarrow CH_3O_2 \rightarrow CH_3O \rightarrow CH_2O$

Table 2
Chemical mechanism for 2,3-pentanedione photolysis.

	Reaction			Rate constant[a]	Reference
1	$CH_3C(O)C(O)C_2H_5 + h\nu$	→	$CH_3CO + C_2H_5CO$	3.6×10^{-5}[c]	This work
2	$CH_3CO + O_2$	→	$CH_3C(O)O_2$	5.1×10^{-12}	Sander et al. (2011)
3	$C_2H_5CO + O_2$	→	$C_2H_5C(O)O_2$	5.1×10^{-12}[b]	Sander et al. (2011)
4	$CH_3C(O)O_2 + CH_3C(O)O_2$	→	$2CH_3O_2 + 2CO_2 + O_2$	1.5×10^{-11}	Sander et al. (2011)
5	$C_2H_5C(O)O_2 + C_2H_5C(O)O_2$	→	$2C_2H_5O_2 + 2CO_2 + O_2$	1.7×10^{-11}	Le Crâne et al. (2005)
6	$CH_3C(O)O_2 + C_2H_5C(O)O_2$	→	$CH_3O_2 + C_2H_5O_2 + 2CO_2 + O_2$	1.5×10^{-11}[b]	Tomas et al. (2000)
7a	$CH_3C(O)O_2 + CH_3O_2$	→	$CH_3O_2 + CH_3O + CO_2 + O_2$	1.1×10^{-11}	Sander et al. (2011)
7b		→	$CH_3C(O)OH + CH_2O + O_2$	$\alpha_7 = 0.9$	Sander et al. (2011)
8a	$C_2H_5C(O)O_2 + CH_3O_2$	→	$C_2H_5O_2 + CH_3O + CO_2 + O_2$	1.1×10^{-11}[b]	Sander et al. (2011)
8b		→	$C_2H_5C(O)OH + CH_2O + O_2$	$\alpha_8 = 0.9$[b]	Sander et al. (2011)
9a	$CH_3C(O)O_2 + C_2H_5O_2$	→	$CH_3O_2 + C_2H_5O + CO_2 + O_2$	1×10^{-11}	Lesclaux (1997)
9b		→	$CH_3C(O)OH + CH_3CHO + O_2$	$\alpha_9 = 0.82$	Lesclaux (1997)
10a	$C_2H_5C(O)O_2 + C_2H_5O_2$	→	$C_2H_5O_2 + C_2H_5O + CO_2 + O_2$	1.2×10^{-11}	Le Crâne et al. (2005)
10b		→	$C_2H_5C(O)OH + CH_3CHO + O_2$	$\alpha_{10} = 0.82$	Le Crâne et al. (2005)
11	$CH_3O + O_2$	→	$CH_2O + HO_2$	1.9×10^{-15}	Sander et al. (2011)
12	$C_2H_5O + O_2$	→	$CH_3CHO + HO_2$	1×10^{-14}	Sander et al. (2011)
13a	$CH_3C(O)O_2 + HO_2$	→	$OH + CH_3O_2 + CO_2$	1.4×10^{-11}	Tomas et al. (2001)
13b		→	$CH_3C(O)OOH + O_2$	$\alpha_{13} = 0.4$	Dillon and Crowley (2008)
13c		→	$CH_3C(O)OH + O_3$	$\beta_{13} = 0.2$	Tomas et al. (2001)
14a	$C_2H_5C(O)O_2 + HO_2$	→	$OH + C_2H_5O_2 + CO_2$	1.4×10^{-11}	Le Crâne et al. (2005)
14b		→	$C_2H_5C(O)OOH + O_2$	$\alpha_{14} = 0.4$[b]	Dillon and Crowley (2008)
14c		→	$C_2H_5C(O)OH + O_3$	$\beta_{14} = 0.2$	Le Crâne et al. (2005)
15	$CH_3O_2 + HO_2$	→	$CH_3OOH + O_2$	5.2×10^{-12}	Sander et al. (2011)
16	$C_2H_5O_2 + HO_2$	→	$C_2H_5OOH + O_2$	8×10^{-12}	Sander et al. (2011)
17	$CH_2O + HO_2$	→	$OHCH_2O_2$	5×10^{-14}	Sander et al. (2011)
−17	$OHCH_2O_2$	→	$CH_2O + HO_2$	125[c]	Veyret et al. (1989)
18	$OH + CH_3C(O)C(O)C_2H_5$	→	$CH_3CHO + CO + CH_3C(O)O_2$	2.09×10^{-12}	Szabo et al. (2011)
19	$OH + CH_2O$	→	$HO_2 + CO + H_2O$	8.5×10^{-12}	Sander et al. (2011)
20	$OH + CH_3CHO$	→	$CH_3C(O)O_2 + H_2O$	1.5×10^{-11}	Sander et al. (2011)
21	$CH_2O + h\nu\ (+O_2)$	→	$HO_2 + CO$	3×10^{-6}[c]	This work

[a] $\alpha_i = k_{ia}/k_i$; $\beta_i = k_{ic}/k_i$ rate constants in cm^3 $molecule^{-1}$ s^{-1}.
[b] Rate constants unavailable in the literature, which were replaced by the rate constants of the corresponding acetyl- or methyl-peroxy radicals reactions.
[c] In s^{-1}.

$C_2H_5CO \rightarrow C_2H_5C(O)O_2 \rightarrow C_2H_5 \rightarrow C_2H_5O_2 \rightarrow C_2H_5O \rightarrow CH_3CHO$

$C_3H_7CO \rightarrow C_3H_7C(O)O_2 \rightarrow C_3H_7 \rightarrow C_3H_7O_2 \rightarrow C_3H_7O \rightarrow C_2H_5CHO$

Corrected (for wall loss and photolysis) yield plots of formaldehyde and acetaldehyde are reported in Fig. 2a for 2,3-pentanedione while corrected yield plots of formaldehyde and propanal are reported in Fig. 2b for 2,3-hexanedione. All plots display linearity and go through the origin, indicating that these products are essentially of primary origin. Table 1 summarizes the corrected product yields obtained in the photolysis of PTD and HEX with and without OH-radical scavenger. It is worth noting that values between 30% and 48% are obtained, well below 100%. This indicates that more than half of the RO_2 radicals arising from the $RC(O)O_2$ (which are produced in the photolysis of the α-diketone, see above) will go into the $RO_2 + HO_2$ terminating reactions, forming hydroperoxides ROOH, while the other half will react with $RC(O)O_2$ radicals, forming the observed carbonyls. The observed yields are thus consistent with the well-known peroxy radical kinetics, where $RO_2 + HO_2$ and $RO_2 + RC(O)O_2$ reaction rate constants are of the same order of magnitude ($\sim 1 \times 10^{-11}$ cm^3 $molecule^{-1}$ s^{-1}, Lesclaux, 1997; Sander et al., 2011). The reported uncertainties in Table 1 correspond only to the statistical uncertainty on the linear regression. Taking into account the statistical uncertainties on the carbonyl product and reactant concentrations, we estimate global uncertainties on the yields of about 20%.

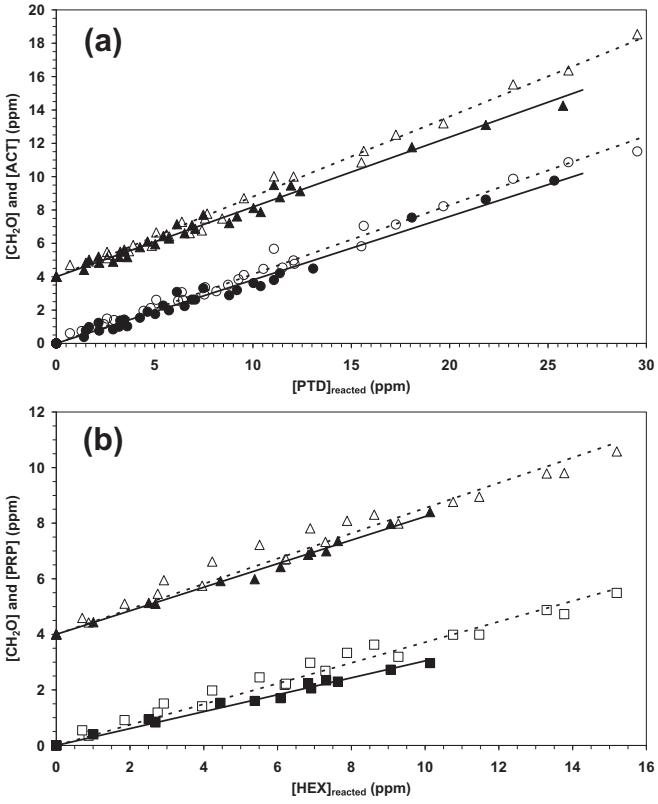

Fig. 2. (a): ACT (○ and ●) and CH_2O (△ and ▲) concentrations produced vs. PTD concentration reacted; (b): Propanal (PRP, ■ and □) and CH_2O (△ and ▲) concentrations produced vs. HEX concentration reacted. Empty symbols are for experiments without OH-scavenger, while full symbols are for experiments with OH-scavenger. The $[CH_2O]$ data have been shifted by +4 for clarity. Dotted lines and full lines correspond to linear fits of the data in the presence and absence of an OH-radical scavenger, respectively.

Looking at Table 1, we note slightly lower carbonyl product yields in the absence of OH scavenger, which could be due to the reaction of OH with the carbonyl products. In the case of 2,3-pentanedione, three different scavengers have been used (1-pentene, ethanol and cyclopentane). In the presence of ethanol, we noted a significant increase in the yield of acetaldehyde (about 50%), which can be attributed to the OH-radical reaction with ethanol (Atkinson, 2000). In the presence of 1-pentene, we observed a significant increase in the yield of formaldehyde (about 58%), which could be due either to the OH-radical reaction with 1-pentene or to the ozonolysis of 1-pentene, both reactions being known to produce CH_2O and butanal (Grosjean and Grosjean, 1996; Atkinson and Arey, 2003). Note that butanal was detected by both GC-FTIR and HPLC-UV analysis, confirming that 1-pentene oxidation took place. These observations strongly suggest the formation of OH-radicals in the mechanism of PTD photolysis, in agreement with the decrease of the photolysis frequency observed in the presence of an OH scavenger. Considering the present knowledge, the only way to form OH radicals appears to be the $RC(O)O_2 + HO_2$ reactions, confirming recent publications (Hasson et al., 2004; Jenkin et al., 2007; Dillon and Crowley, 2008).

Small amounts of CO have also been detected by FTIR spectroscopy. As shown in Fig. 3, the plots of CO vs. reacted α-diketone are not linear but follow roughly a second order polynomial, indicating multiple CO formation processes. The average molar yields of carbon monoxide determined by the derivative of the curves at the origin in the absence and presence of cyclopentane are (7.6 ± 0.5)% and (2.6 ± 0.1)%, respectively, for PTD, and (7.1 ± 0.1)% and (1.7 ± 0.3)%, respectively, for HEX. Global uncertainties are of the order of 20% for the values without scavenger, and 30% for the values with scavenger (because of lower CO amounts measured and scavenger interferences in the IR spectra).

As for the carbonyl products, the significant difference in the CO yields with and without OH scavenger may be attributed to the OH radicals reacting with α-diketone and leading to CO formation. The following hypothetical mechanism (shown for PTD) is suggested:

$CH_3C(O)C(O)CH_2CH_3 + OH \rightarrow CH_3C(O)C(O)CHCH_3 + H_2O$

$CH_3C(O)C(O)CHCH_3 + O_2 \rightarrow CH_3C(O)C(O)C(O_2)HCH_3$

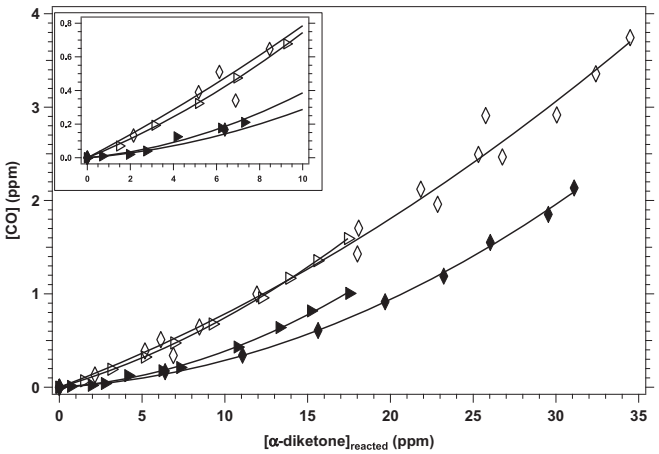

Fig. 3. CO produced vs. PTD (diamonds) or HEX (triangles) reacted in the absence (◇,▷) and presence (◆,▶) of cyclopentane as OH-radical scavenger. The lines correspond to second-order fit of the data. The insert shows a zoom on the first experimental data.

$CH_3C(O)C(O)C(O_2)HCH_3 + RO_2 \rightarrow CH_3C(O)C(O)COHCH_3 + RO + O_2$

$CH_3C(O)C(O)COHCH_3 \rightarrow CH_3CO + CO + CH_3CHO$

Thus, the relatively high formation yields of CO in the absence of OH-radical scavenger also support the formation of OH radicals in the reaction mechanism. The processes responsible for the secondary formation of CO and the curved CO yield plots are thought to be principally the photolysis of formaldehyde and its reaction with OH (Atkinson et al., 2006).

3.4. Chemical mechanism simulations

From our observations, it is possible to develop a reaction mechanism for the photolysis of 2,3-pentanedione and 2,3-hexanedione. The calculation of the C–C bond energies from the formation enthalpies (Jagiella and Zabel, 2008; Kercher et al., 2005; Sander et al., 2011) as well as the observation of very small CO formation yields near time zero (in the presence of an OH-scavenger) suggest that the first step after the absorption of a photon is mainly the rupture of the C(O)–C(O) bond of the molecule. At atmospheric pressure, acyl radicals react rapidly with oxygen to form acyl peroxy radicals $RC(O)O_2$ (Atkinson et al., 2006; Tomas et al., 2000): acetyl $CH_3C(O)O_2$ and propionyl $CH_3CH_2C(O)O_2$ peroxy radicals for PTD, and acetyl and n-butyryl $CH_3CH_2CH_2C(O)O_2$ radicals for HEX. In the absence of NO_x, the acyl peroxy radicals react with other peroxy radicals to form radicals as well as stable carbonyl, organic acid and peroxide species. Based on the present knowledge on peroxy radical reaction kinetics and mechanisms (Le Crâne et al., 2005; Lesclaux, 1997; Sander et al., 2011; Tomas and Lesclaux, 2000; Tyndall et al., 2001), a chemical mechanism for 2,3-pentanedione photolysis has been built (Table 2). A very similar chemical mechanism was developed for 2,3-hexanedione (Table S1). Self- and cross- RO_2 reactions have been neglected due to their very low rate constants ($<3.7 \times 10^{-13}$ cm^3 $molecule^{-1}$ s^{-1}, Lesclaux, 1997). Molecular channels leading to the formation of carboxylic acids (reactions 7b, 8b, 9b, 10b, 13c and 14c) have low branching ratios (of the order of 0.1–0.2) (Le Crâne et al., 2005; Lesclaux, 1997; Sander et al., 2011; Tomas et al., 2001). Note that small amounts of acetic, propanoïc, and butanoïc acids were detected by ion chromatography–mass spectrometry, with estimated yields of about 10% each. Recent studies have shown that acyl peroxy radicals react with HO_2 according to three channels, one leading to OH and RO_2 radicals with a branching ratio of about 0.4–0.5, the two others being molecular channels producing a hydroperoxide for the first one (with a

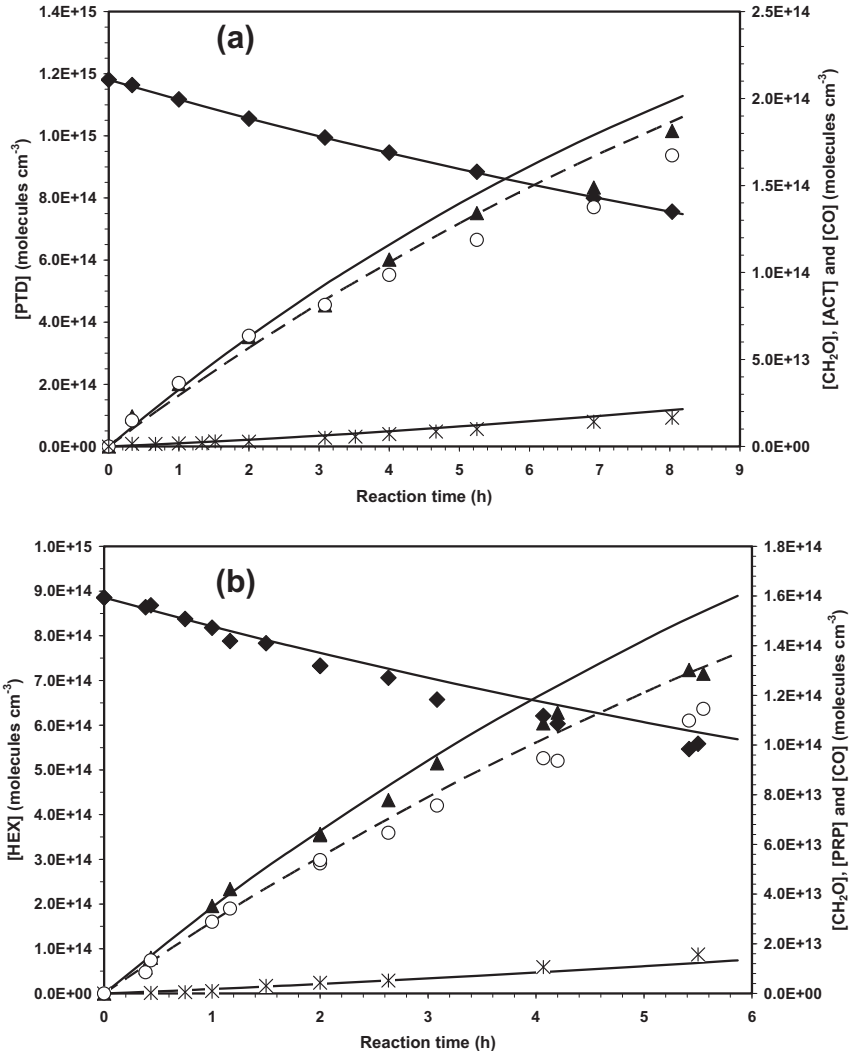

Fig. 4. Experimental and simulated temporal profiles for (a): PTD and (b): HEX photolysis. (◆): PTD and HEX; (▲): CH_2O; (○): ACT and propanal (PRP) and (*): CO. Left axis: reactant concentrations; right axis: product concentrations. Dotted lines correspond to ACT and PRP data.

branching ratio of about 0.4) and organic acid + ozone (with a branching ratio of about 0.2) for the second one (Dillon and Crowley, 2008; Hasson et al., 2004; Jenkin et al., 2007; Le Crâne et al., 2005; Tomas et al., 2001). Finally, the equilibrated reaction between HO_2 and CH_2O was taken into account (Veyret et al., 1989; Morajkar et al., 2013), while those between HO_2 and higher aldehydes were considered of minor importance under the present conditions (Tomas et al., 2001).

Time profiles for the reactant and the observed products were simulated in the case of experiments with OH scavenger only, using the developed chemical mechanism and integrating the kinetic differential equations with the Euler method. In the case of experiments without OH scavenger, as OH radicals (supposed to be formed) will react with reactant and products leading to much more complex reaction systems, it was not attempted to simulate the corresponding temporal profiles. All the rate constants and branching ratios were taken from the literature and are known with a relatively good precision. Input data include the initial α-diketone concentration as well as the α-diketone photolysis constant, which was slightly adjusted to fit the data (±10%). Fig. 4a and b illustrate the resulting profiles for 2,3-pentanedione and 2.3-hexanedione. Very good agreement was obtained for PTD and HEX. In the case of HEX, the model slightly overestimates (by about 15%) the observed CH_2O and propanal concentrations after 6 h photolysis, which could be due to the larger uncertainties in the HEX concentrations compared to those of PTD due to analytical interferences between 2,3-hexanedione and cyclopentane (OH scavenger).

Organic acid yields can also be retrieved from the numerical simulations. Equal yields of 13% have been determined for acetic, propanoïc, and butanoïc acids, consistent with the estimations of 10% from the ion chromatography analysis. RC(O)OH species come from $RC(O)O_2$ reactions with either RO_2 or HO_2 radicals through the molecular channel with similar rate constants (1.1 and 1.4×10^{-11}) and branching ratios (~0.2) (Sander et al., 2011). These peroxy radical reactions compete with $RC(O)O_2 + R'C(O)O_2$ reactions (rate constant of 1.6×10^{-11} cm^3 $molecule^{-1}$ s^{-1}) (Sander et al., 2011). Thus, the obtained yields appear consistent with the higher $RC(O)O_2 + R'C(O)O_2$ reaction rates.

3.5. Atmospheric implications

The photolysis frequencies determined in the present work (paragraph 3.1) are specific to the experimental setup used and cannot be directly applied for the estimation of the atmospheric lifetime. The values of the photolysis rate constant of the α-diketone corresponding to atmospheric conditions ($k^{atm}_{\alpha-diketone}$) can be determined using the photolysis frequency of NO_2 in the troposphere ($k^{atm}_{NO_2}$) through the following equation:

$$k^{atm}_{\alpha-diketone} = k_{\alpha-diketone} \times \frac{k^{atm}_{NO_2}}{k_{NO_2}}$$

On 1st July at noon, 40 °N and with cloudless sky, the rate coefficient $k^{atm}_{NO_2}$ rates at 29 h^{-1} (Seinfeld and Pandis, 1998). Using the photolysis frequency values of α-diketone ($k_{\alpha-diketone}$) and NO_2 (k_{NO_2}) measured in the reaction chamber allows to calculate the photolysis frequencies of PTD and HEX in the troposphere: $k^{atm}_{PTD} = 0.42$ h^{-1} and $k^{atm}_{HEX} = 0.38$ h^{-1}. The atmospheric lifetime of 2,3-pentanedione and 2,3-hexanedione can then be retrieved according to

$$\tau^{atm}_{\alpha-diketone} = \frac{1}{k^{atm}_{\alpha-diketone}}$$

Relatively short tropospheric lifetimes of about 2.4 h for the PTD and 2.6 h for the HEX are obtained, confirming the dominant role of photolysis in the fate of α-dicarbonyl species. These values are in agreement with the rough estimation of 1 h by Szabo et al. (2011) based on the absorption cross sections and an assumed average quantum yield of 0.1. The calculated lifetimes are also of the same order of magnitude as the photolysis lifetime of other α-dicarbonyls: 3–5 h for glyoxal (Plum et al., 1983; Tadic et al., 2006), 2–4 h for methylglyoxal (Koch and Moortgat, 1998; Plum et al., 1983) and 1 h for biacetyl (Calvert et al., 2011). Reaction of PTD with OH in the atmosphere has been shown to be less important with a lifetime of 5.3 days (Szabo et al., 2011). Local impacts should thus be expected for such α-dicarbonyl compounds with direct formation of radicals which will contribute to the oxidative capacity of the troposphere. To our best knowledge, the present kinetic photolysis study is the first determination of tropospheric lifetime and fate of 2,3-hexanedione and the first study of 2,3-pentanedione photolysis products.

Acknowledgments

Our laboratory participates in the Institut de Recherche en ENvironnement Industriel (IRENI), which is financed by the Communauté Urbaine de Dunkerque, the Nord-Pas de Calais Regional Council, the French Ministry of Higher Education and Research, the CNRS and the European Regional Development Fund. The present work also takes place in the Labex CaPPA (Chemical and Physical Properties of the Atmosphere) supported by the French research agency ANR. H. Bouzidi is grateful for a PhD scholarship from the Nord-Pas de Calais Regional Council and Mines Douai.

Appendix A. Supplementary data

Supplementary data related to this article can be found at http://dx.doi.org/10.1016/j.atmosenv.2013.10.039.

References

Atkinson, R., 2000. Atmospheric chemistry of VOCs and NOx. Atmos. Environ. 34, 2063–2101.
Atkinson, R., Arey, J., 2003. Atmospheric degradation of volatile organic compounds. Chem. Rev. 103, 4605–4638.
Atkinson, R., Baulch, D.L., Cox, R.A., Crowley, J.N., Hampson, R.F., Hynes, R.G., Jenkin, M.E., Rossi, M.J., Troe, J., 2004. Evaluated kinetic and photochemical data for atmospheric chemistry: volume I–gas phase reactions of O_x, HO_x, NO_x and SO_x species. Atmos. Chem. Phys. 4, 1461–1738.
Atkinson, R., Baulch, D.L., Cox, R.A., Crowley, J.N., Hampson, R.F., Hynes, R.G., Jenkin, M.E., Rossi, M.J., Troe, J., 2006. Evaluated kinetic and photochemical data for atmospheric chemistry: volume II. Gas phase reactions of organic species. Atmos. Chem. Phys. 6, 3625–4055.
Calvert, J.G., Atkinson, R., Becker, K.H., Kamens, R.M., Seinfeld, J.H., Wallington, T.J., Yarwood, G., 2002. The Mechanisms of Atmospheric Oxidation of Aromatic Hydrocarbons. Oxford University Press, New York.
Calvert, J.G., Mellouki, A., Orlando, J.J., Pilling, M.J., Wallington, T.J., 2011. The Mechanisms of Atmospheric Oxidation of the Oxygenates. Oxford University Press, New York.
Campo, E., Ferreira, V., Escudero, A., Marqués, J.C., Cacho, J., 2006. Quantitative gas chromatography–olfactometry and chemical quantitative study of the aroma of four Madeira wines. Anal. Chim. Acta 563, 180–187.
Dillon, T.J., Crowley, J.N., 2008. Direct detection of OH formation in the reactions of HO_2 with $CH_3C(O)O_2$ and other substituted peroxy radicals. Atmos. Chem. Phys. 8, 4877–4889.
Djehiche, M., Tomas, A., Fittschen, C., Coddeville, P., 2011. First cavity ring-down spectroscopy HO_2 measurements in a large photoreactor. Z. Phys. Chem. 225, 983–992.
Fu, T.-M., Jacob, D.J., Wittrock, F., Burrows, J.P., Vrekoussis, M., Henze, D.K., 2008. Global budgets of atmospheric glyoxal and methylglyoxal, and implications for formation of secondary organic aerosols. J. Geophys. Res. 113.
Grosjean, E., Grosjean, D., 1996. Carbonyl products of the gas-phase reaction of ozone with 1-alkenes. Atmos. Environ. 30, 4107–4113.
Grosjean, E., Grosjean, D., 1998. The gas-phase reaction of alkenes with ozone: formation yields of carbonyls from biradicals in ozone-alkene-cyclohexane experiments. Atmos. Environ. 32, 3393–3402.

Hamilton, J.F., Webb, P.J., Lewis, A.C., Reviejo, M.M., 2005. Quantifying small molecules in secondary organic aerosol formed during the photo-oxidation of toluene with hydroxyl radicals. Atmos. Environ. 39, 7263–7275.

Hasson, A.S., Tyndall, G.S., Orlando, J.J., 2004. A product yield study of the reaction of HO_2 radicals with ethyl peroxy ($C_2H_5O_2$), acetyl peroxy ($CH_3C(O)O_2$), and acetonyl peroxy ($CH_3C(O)CH_2O_2$) radicals. J. Phys. Chem. A 108, 5979–5989.

Holmes, J.R., O'Brien, R.J., Crabtree, J.H., Hecht, T.A., Seinfeld, J.H., 1973. Measurement of ultraviolet radiation intensity in photochemical smog studies. Environ. Sci. Technol. 7, 519–523.

Jagiella, S., Zabel, F., 2008. Thermal stability of carbonyl radicals. Part II. Reactions of methylglyoxyl and methylglyoxylperoxy radicals at 1 bar in the temperature range 275–311 K. Phys. Chem. Chem. Phys. 10, 1799–1808.

Jenkin, M.E., Hurley, M.D., Wallington, T.J., 2007. Investigation of the radical product channel of the $CH_3C(O)O_2 + HO_2$ reaction in the gas phase. Phys. Chem. Chem. Phys. 9, 3149–3162.

Kercher, J.P., Fogleman, E.A., Koizumi, H., Sztáray, B., Baer, T., 2005. Heats of formation of the propionyl ion and radical and 2,3-pentanedione by threshold photoelectron photoion coincidence spectroscopy. J. Phys. Chem. A 109, 939–946.

Klotz, B., Graedler, F., Sorensen, S., Barnes, I., Becker, K.H., 2001. A kinetic study of the atmospheric photolysis of α-dicarbonyls. Int. J. Chem. Kinet. 33, 9–20.

Koch, R., Moortgat, G.K., 1998. Photochemistry of methylglyoxal in the vapor phase. J. Phys. Chem. A 102, 9142–9153.

Le Crâne, J.-P., Villenave, E., Hurley, M.D., Wallington, T.J., Ball, J.C., 2005. Atmospheric chemistry of propionaldehyde: kinetics and mechanisms of reactions with OH radicals and Cl atoms, UV spectrum, and self-reaction kinetics of $CH_3CH_2C(O)O_2$ radicals at 298 K. J. Phys. Chem. A 109, 11837–11850.

Lesclaux, R., 1997. Combination of Peroxyl Radicals in the Gas Phase. Peroxyl Radicals. Z. B. Alfassi. John Wiley & Sons Ltd., New York, pp. 81–112.

Morajkar, P., Schoemaecker, C., Okumura, M., Fittschen, C., 2013. Direct measurement of the equilibrium constants of the reaction of formaldehyde and acetaldehyde with HO_2 radicals. Int. J. Chem. Kinet. http://dx.doi.org/10.1002/kin.20817.

Plum, C.N., Sanhueza, E., Atkinson, R., Carter, W.P.L., Pitts, J.N., 1983. OH radical rate constants and photolysis rates of α-dicarbonyls. Environ. Sci. Technol. 17, 479–484.

Sander, S.P., Abbatt, J.P.D., Barker, J.R., Burkholder, J.B., Friedl, R.R., Golden, D.M., Huie, R.E., Kolb, C.E., Kurylo, M.J., Moortgat, G.K., Orkin, V.L., Wine, P.H., 2011. Chemical Kinetics and Photochemical Data for Use in Atmospheric Studies, Evaluation No. 17. Jet Propulsion Laboratory, Pasadena. http://jpldataeval.jpl.nasa.gov.

Seinfeld, J.H., Pandis, S.N., 1998. Atmospheric Chemistry and Physics. John Wiley & Sons.

Szabo, E., Djehiche, M., Riva, M., Fittschen, C., Coddeville, P., Sarzynski, D., Tomas, A., Dobé, S., 2011. Atmospheric chemistry of 2,3-pentanedione: photolysis and reaction with OH radicals. J. Phys. Chem. A 115, 9160–9168.

Szabo, E., Tarmoul, J., Tomas, A., Fittschen, C., Dobe, S., Coddeville, P., 2009. Kinetics of the OH-radical initiated reactions of acetic acid and its deuterated isotopes. React. Kinet. Catal. Lett. 96, 299–309.

Tadic, J., Moortgat, G.K., Wirtz, K., 2006. Photolysis of glyoxal in air. J. Photochem. Photobiol. A 177, 116–124.

Tomas, A., Lesclaux, R., 2000. Self-reaction kinetics of the $(CH_3)_2CHC(O)O_2$ and $(CH_3)_3CC(O)O_2$ acylperoxy radicals between 275 and 363 K. Chem. Phys. Lett. 319, 521–528.

Tomas, A., Villenave, E., Lesclaux, R., 2000. Kinetics of the $(CH_3)_2CHCO$ and $(CH_3)_3CCO$ radical decomposition: temperature and pressure dependences. Phys. Chem. Chem. Phys. 2, 1165–1174.

Tomas, A., Villenave, E., Lesclaux, R., 2001. Reactions of the HO_2 radical with CH_3CHO and $CH_3C(O)O_2$ in the gas phase. J. Phys. Chem. A 105, 3505–3514.

Turpin, E., Tomas, A., Fittschen, C., Devolder, P., Galloo, J.-C., 2006. Acetone-h_6 or -d_6 + OH reaction products: evidence for heterogeneous formation of acetic acid in a simulation chamber. Environ. Sci. Technol. 40, 5956–5961.

Tyndall, G.S., Cox, R.A., Granier, C., Lesclaux, R., Moortgat, G.K., Pilling, M.J., Ravishankara, A.R., Wallington, T.J., 2001. Atmospheric chemistry of small organic peroxy radicals. J. Geophys. Res. 106, 12157–12182.

Veyret, B., Lesclaux, R., Rayez, M.T., Rayez, J.C., Cox, R.A., Moortgat, G.K., 1989. Kinetics and mechanism of the photo-oxidation of formaldehyde. 1. Flash photolysis study. J. Phys. Chem. 93, 2368–2374.